

# RSC Advances



This is an *Accepted Manuscript*, which has been through the Royal Society of Chemistry peer review process and has been accepted for publication.

*Accepted Manuscripts* are published online shortly after acceptance, before technical editing, formatting and proof reading. Using this free service, authors can make their results available to the community, in citable form, before we publish the edited article. This *Accepted Manuscript* will be replaced by the edited, formatted and paginated article as soon as this is available.

You can find more information about *Accepted Manuscripts* in the [Information for Authors](#).

Please note that technical editing may introduce minor changes to the text and/or graphics, which may alter content. The journal's standard [Terms & Conditions](#) and the [Ethical guidelines](#) still apply. In no event shall the Royal Society of Chemistry be held responsible for any errors or omissions in this *Accepted Manuscript* or any consequences arising from the use of any information it contains.

## ARTICLE

# Transport properties and enhanced thermoelectric performance of aluminum doped $\text{Cu}_3\text{SbSe}_4$

Cite this: DOI: 10.1039/x0xx00000x

Yuanyue Li<sup>a</sup>, Xiaoying Qin<sup>a\*</sup>, Di Li<sup>a\*</sup>, Xiyu Li<sup>a</sup>, Yongfei Liu<sup>a</sup>, Jian Zhang<sup>a</sup>, Chunjun Song<sup>a</sup> and Hongxing Xin<sup>a</sup>

<sup>a</sup>Key Laboratory of Materials Physics, Institute of Solid State Physics, Chinese Academy of Sciences, 230031 Hefei, People's Republic of China

Received 00th January 2012,  
Accepted 00th January 2012

\*Corresponding author: [xyqin@issp.ac.cn](mailto:xyqin@issp.ac.cn), [lidi@issp.ac.cn](mailto:lidi@issp.ac.cn)

DOI: 10.1039/x0xx00000x

[www.rsc.org/](http://www.rsc.org/)

## Abstract

The electrical transport and thermoelectric properties of  $\text{Cu}_3\text{Sb}_{1-x}\text{Al}_x\text{Se}_4$  ( $x = 0, 0.01, 0.02$  and  $0.03$ ) compounds are investigated in the temperatures range of 300–600 K. The results indicate that with increasing Al content from  $x = 0$  to  $x = 0.03$  hole concentration increases monotonically from  $8.04 \times 10^{17}$  to  $1.19 \times 10^{19} \text{ cm}^{-3}$  due to the substitution of  $\text{Al}^{3+}$  for  $\text{Sb}^{5+}$ , thus leading to a large decrease in the electrical resistivity of  $\text{Cu}_3\text{Sb}_{1-x}\text{Al}_x\text{Se}_4$ . Meanwhile, the increase in hole concentration leads to a transition from non-degenerate ( $x = 0$ ) to partial degenerate ( $x = 0.01, 0.02$ ) and then to degenerate state ( $x = 0.03$ ). Power factor (PF) of all the Al-doped  $\text{Cu}_3\text{Sb}_{1-x}\text{Al}_x\text{Se}_4$  samples is remarkably improved due to the optimization of hole concentration. Lattice thermal conductivity  $\kappa_L$  of the heavily doped sample ( $x = 0.03$ ) is reduced. As a result, a large thermoelectric figure of merit  $ZT = 0.58$  is obtained for  $\text{Cu}_3\text{Sb}_{0.97}\text{Al}_{0.03}\text{Se}_4$  at 600 K, which is around 1.9 times as large as that of the un-doped  $\text{Cu}_3\text{SbSe}_4$ .

## 1. Introduction

Thermoelectric (TE) materials have attracted more and more attention because of their applications as power generators and heat pumps<sup>[1]</sup>. The efficiency of a TE material is generally characterized by the dimensionless figure of merit  $ZT$ , defined as  $ZT = (S^2T)/\rho(\kappa_C + \kappa_L)$ , where  $\rho$ ,  $S$ ,  $\kappa_C$ ,  $\kappa_L$  and  $T$  are the electrical resistivity, Seebeck coefficient, thermal conductivity from carrier contribution, lattice thermal conductivity and absolute temperature, respectively<sup>[2]</sup>. Copper-based multinary semiconductors have recently received much attention due to their good electronic transport properties and relatively low intrinsic thermal conductivity, which contributes to being good TE materials (e.g.  $\text{Cu}_{2.10}\text{Cd}_{0.90}\text{SnSe}_4$ ,  $ZT = 0.65$  at 700 K,  $\text{Cu}_2\text{Sn}_{0.90}\text{In}_{0.10}\text{Se}_3$ ,  $ZT = 1.14$  at 850 K,  $\text{Cu}_3\text{Sb}_{0.97}\text{Ge}_{0.03}\text{Se}_{2.8}\text{S}_{1.2}$ ,  $ZT = 0.89$  at 650 K)<sup>[3–10]</sup>.

The ternary semiconductor of  $\text{Cu}_3\text{SbSe}_4$ , as a narrow band gap semiconductor (0.13–0.42 eV)<sup>[11]</sup> with a unit cell four times larger than  $\text{ZnSe}$  ( $n = 8$  for  $\text{Cu}_3\text{SbSe}_4$  versus  $n = 2$  for  $\text{ZnSe}$ ), was firstly synthesized by Wernick and Benson<sup>[12]</sup> with high Seebeck coefficient and low thermal conductivity at room temperature (the Cu/Se atoms form the structural framework and the rest Sb atoms have the rattling behaviors similar to the resonators<sup>[13]</sup>). However, the un-doped  $\text{Cu}_3\text{SbSe}_4$  compound has low hole concentration and relatively large electrical resistivity, which leads to low TE performance. As reported in early work<sup>[14]</sup>, the  $ZT$  of  $\text{Cu}_3\text{SbSe}_4$  is too small to be used in practice. Hence, it is a key issue to reduce its electrical resistivity and to optimize its PF ( $PF = S^2/\rho$ ). Earlier work done by Skoug et al. showed that doping with either Ge or Sn at the Sb site can improve the thermoelectric performance of  $\text{Cu}_3\text{SbSe}_4$ <sup>[15]</sup>.

Wei et al.<sup>[16]</sup> present a quite systematic study of  $\text{Cu}_3\text{SbSe}_4$ , which is done in advance of current work, and have achieved promising  $ZT = \sim 0.7$  at 673 K for  $\text{Cu}_3\text{Sb}_{0.98}\text{Sn}_{0.02}\text{Se}_4$ .

In our previous work<sup>[17]</sup>, we showed that the thermoelectric performance of  $\text{Cu}_3\text{SbSe}_4$  could be improved by doping the element Bi, where the equivalent substitution of  $\text{Sb}^{5+}$  with  $\text{Bi}^{5+}$  led to a limited increase in the hole concentration. In the present work, Al, a cheap, environment-friendly and abundant element, is used as the dopant and the inequitable substitution of  $\text{Al}^{3+}$  for  $\text{Sb}^{5+}$  will introduce hole into the host, giving rise to a large increase in hole concentration in this p-type compound  $\text{Cu}_3\text{SbSe}_4$ . Our experiments demonstrate that Al-doping can effectively adjust the hole concentration and optimize PF. Moreover,  $\kappa_L$  of the heavily doped sample ( $x = 0.03$ ) is reduced. As a result,  $ZT = 0.58$  is achieved for  $\text{Cu}_3\text{Sb}_{0.97}\text{Al}_{0.03}\text{Se}_4$  at 600 K, which is about 1.9 times larger than that of the  $\text{Cu}_3\text{SbSe}_4$ .

## 2. Experimental

Samples of  $\text{Cu}_3\text{Sb}_{1-x}\text{Al}_x\text{Se}_4$  ( $x = 0, 0.01, 0.02$  and  $0.03$ ) were prepared by direct melting of the pure elements (Cu, 99.99%; Sb, 99.99%; Al, 99.99%; Se, 99.99%) in evacuated quartz ampoules that were pumped under vacuum of  $10^{-2}$  Pa. Before that, the quartz ampoules were under ultrasonic treatment for two hours to insure the cleanliness of the surface. The samples were placed in a digitally controlled furnace and slowly heated ( $20^\circ\text{C/h}$ ) for 2700 min up to  $900^\circ\text{C}$ , held for 12 hours, then cooled to  $500^\circ\text{C}$  ( $1^\circ\text{C/min}$ ) and quenched in water at room temperature. After quenching, the samples were annealed at  $300^\circ\text{C}$  for 48 hours to promote

homogeneity. The resulted ingots were pulverized into powders (The size distribution is around 1–2  $\mu\text{m}$ ) in an agate mortar. The bulk samples were obtained by spark plasma sintering (SPS) for 5 min at the temperature of 673 K under the pressure of 50 MPa. In each charge for the SPS machine, about 4.5 g powders were employed.

The phase of the obtained samples was checked by using x-ray diffraction (Philips diffractometer,  $\text{Cu K}\alpha$  radiation). The specimens for transport measurements were cut from the bulk samples by using a diamond saw. Electrical resistivity and Seebeck coefficient were measured by the ZEM-3 system from ULVAC. The thermal diffusivity,  $D$ , was measured using the laser flash method (Netzsch, LFA-457). The specific heat,  $C_p$ , was determined by differential scanning calorimetry (DSC Pyris Diamond). The resulting thermal conductivity was calculated from the measured thermal diffusivity  $D$ , specific heat  $C_p$ , and density  $d$  from the relationship  $\kappa = DdC_p$ . The density of the bulk materials was measured by Archimedes' methods using alcohol as the medium, and all were above 90% of the theory density, as shown in Table 1. Thin plate samples were used for Hall measurements, which were conducted by CVM-200 Hall effect measurement system.

### 3. Result and discussions

The XRD patterns of all the samples  $\text{Cu}_3\text{Sb}_{1-x}\text{Al}_x\text{Se}_4$  ( $x = 0, 0.01, 0.02$  and  $0.03$ ) at room temperature are shown in Fig. 1. The main diffraction peaks correspond well to the standard JCPDS card (No. 01-085-0003) of  $\text{Cu}_3\text{SbSe}_4$  with tetragonal structure (space group I-42m,  $a = 5.661 \text{ \AA}$ ,  $c = 11.28 \text{ \AA}$ )<sup>[13]</sup>, indicating that the doped specimens have the same crystallographic structure as that of the  $\text{Cu}_3\text{SbSe}_4$  phase and no obvious impurity phase is observed. A

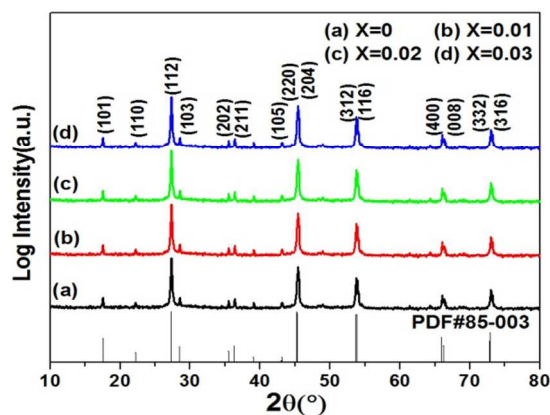


Fig. 1 XRD patterns at room temperature for  $\text{Cu}_3\text{Sb}_{1-x}\text{Al}_x\text{Se}_4$  samples: (a)  $x = 0$ , (b)  $x = 0.01$ , (c)  $x = 0.02$  and (d)  $x = 0.03$ .

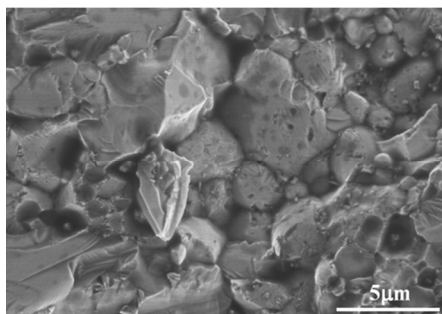


Fig. 2 SEM image of fracture surface of bulk sample  $\text{Cu}_3\text{Sb}_{0.97}\text{Al}_{0.03}\text{Se}_4$ .

Reitveld refinement approach is employed to calculate the lattice parameters from the XRD data. The result reveals that lattice parameters  $a$  and  $c$  decrease monotonically with increasing Al content, as shown in Table I, which is due to the substitution of  $\text{Al}^{3+}$  with smaller ionic radius (0.39  $\text{\AA}$ ) for  $\text{Sb}^{5+}$  possessing larger ionic radius (0.62  $\text{\AA}$ ).

Fig. 2 shows the SEM image of fracture surface of bulk sample  $\text{Cu}_3\text{Sb}_{0.97}\text{Al}_{0.03}\text{Se}_4$ . One can see from the image that the typical grain sizes are in the range of 1–5  $\mu\text{m}$ . In addition, there are a large number of nanoparticles embedded at grain boundaries, indicating that the dispersed distribution of the nanoparticles will be beneficial to inhibiting lattice thermal conductivity of the bulk specimens due to extra enhanced phonon scattering. Our observation indicates that the nanoparticles exist in both doped samples and un-doped samples (not shown here).

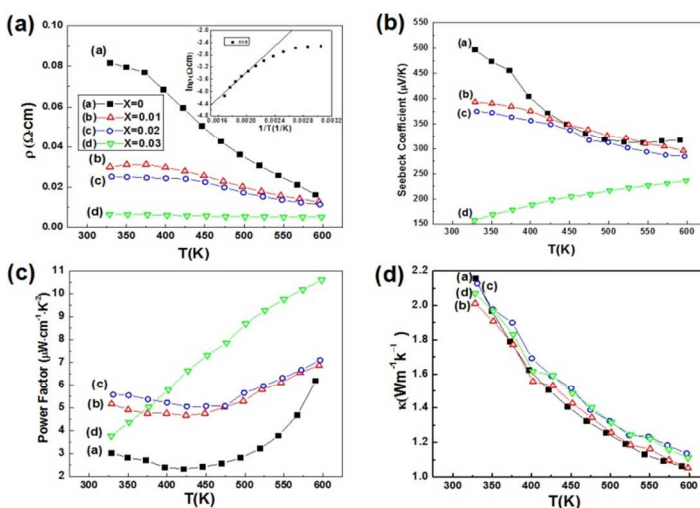


Fig. 3 Temperature dependences of (a) electrical resistivity, (b) Seebeck coefficient, (c) power factor, and (d) total thermal conductivity for  $\text{Cu}_3\text{Sb}_{1-x}\text{Al}_x\text{Se}_4$ : (a)  $x = 0$ , (b)  $x = 0.01$ , (c)  $x = 0.02$  and (d)  $x = 0.03$ . The inset of (a) is the logarithmic plot of  $\rho$  versus  $1/T$  for  $\text{Cu}_3\text{SbSe}_4$ .

The thermoelectric properties of  $\text{Cu}_3\text{Sb}_{1-x}\text{Al}_x\text{Se}_4$  ( $x = 0, 0.01, 0.02$  and  $0.03$ ) are shown in Fig. 3. As displayed in Fig. 3(a), the electrical resistivity  $\rho$  of  $\text{Cu}_3\text{SbSe}_4$  decreases with increasing temperature, indicating that the un-doped sample exhibits semiconductor-like behavior. However, in the case of the Al-doped compounds,  $\rho$  shows different temperature dependences.  $\rho$  of sample with  $x = 0.01$  initially increases slightly with increasing temperature and reaches a peak value of  $3.12 \times 10^{-4} \Omega \cdot \text{m}$  at 375 K and then decreases with further increasing temperature. With increasing Al content to  $x = 0.02$ ,  $\rho$  almost remains the same value in the temperature range from 325 K to 375 K and then decreases with further increasing temperature, reaching  $1.3 \times 10^{-4} \Omega \cdot \text{m}$  at 600 K which is comparable to that of the sample with  $x = 0.01$ . However,  $\rho$  in the case with  $x = 0.03$  almost remains unchanged in the whole temperature range. In addition, Al doping causes the decrease in the magnitude of the electrical resistivity.

In order to examine the temperature behavior of the resistivity for  $\text{Cu}_3\text{SbSe}_4$ , logarithm of the resistivity  $\rho$  as a function of reciprocal of temperature is given in the inset of Fig. 3(a). It can be seen that good linear relationships between  $\ln \rho$  and  $1/T$  exist in the high temperature range for  $\text{Cu}_3\text{SbSe}_4$ . The existence of a linear

relationship between  $\ln\rho$  and  $1/T$  means that the resistivity can be described by using a thermally activated expression in corresponding temperature regimes, written as:

$$\ln \rho = C + \frac{E_g}{2k_B T} \tag{1}$$

where  $C$  is an consistent and  $k_B$  Boltzmann constant,  $E_g$  band gap. By best fitting of the experimental data to formula (1), one can obtain  $E_g = 0.3$  eV for  $\text{Cu}_3\text{SbSe}_4$ , which is almost equal to the energy gap  $E_g = 0.29$  eV for  $\text{Cu}_3\text{SbSe}_4$  reported by Wei et al.<sup>[16]</sup>, indicating that the un-doped sample is an intrinsic semiconductor. The activation energy  $E_a = E_g/2 = 0.15$  eV, which is similar to the result (0.13 eV) of Wei et al.<sup>[16]</sup> determined from resistivity.

Our further measurements (see following text) demonstrate that Seebeck coefficient and Hall coefficient of  $\text{Cu}_3\text{SbSe}_4$  are positive in the whole temperature investigated, indicating the major carriers are holes. Since the substitution of  $\text{Al}^{3+}$  for  $\text{Sb}^{5+}$  occurs, the doping of Al is expected to introduce holes into the host. Therefore, the Al substitution for Sb will give rise to a large increase in hole concentration. The hole concentrations  $p$  at room temperature for  $\text{Cu}_3\text{Sb}_{1-x}\text{Al}_x\text{Se}_4$  ( $x = 0, 0.01, 0.02$  and  $0.03$ ) are calculated according to the measured Hall coefficient and the results are listed in Table 1. One can see that the hole concentration increases from  $8.04 \times 10^{17} \text{ cm}^{-3}$  for  $x = 0$  to  $2.50 \times 10^{18} \text{ cm}^{-3}$  for  $x = 0.01$ ,  $4.12 \times 10^{18} \text{ cm}^{-3}$  for  $x = 0.02$  and  $1.19 \times 10^{19} \text{ cm}^{-3}$  for  $x = 0.03$ , respectively. Al-doping leads to the increase in hole concentration, which explains the smaller resistivity upon doping.

Table 1  
List of lattice parameters (a and c), Hall mobility  $\mu$ , carrier concentration  $p$  and relative density  $d_r$  at room temperature for  $\text{Cu}_3\text{Sb}_{1-x}\text{Al}_x\text{Se}_4$  ( $x = 0, 0.01, 0.02$  and  $0.03$ ).

$\text{Cu}_3\text{Sb}_{1-x}\text{Al}_x\text{Se}_4$	$a(\text{\AA})^a$	$c(\text{\AA})^b$	$\mu(\text{cm}^2\text{V}^{-1}\text{s}^{-1})^c$	$p(\text{cm}^{-3})^d$	$d_r(\%)^e$
$x = 0$	5.654	11.196	94.1	$8.04 \times 10^{17}$	91
$x = 0.01$	5.635	11.175	83.0	$2.50 \times 10^{18}$	91
$x = 0.02$	5.618	11.156	61.0	$4.12 \times 10^{18}$	92
$x = 0.03$	5.601	11.137	52.5	$1.19 \times 10^{19}$	91

<sup>a</sup> $a$  and <sup>b</sup> $c$  are lattice parameters.

<sup>c</sup> $\mu$  is Hall mobility.

<sup>d</sup> $p$  is carrier concentration

<sup>e</sup> $d_r$  is relative density, defined as  $d_r = d/d_0$ , where  $d$  is measured density of samples and  $d_0 (= 5.86 \text{ g/cm}^3)$  is theoretical density of  $\text{Cu}_3\text{SbSe}_4$ .

All the samples are p-type semiconductors, as verified by the positive Seebeck coefficients, which are shown in Fig. 3(b). The Seebeck coefficient  $S$  for  $\text{Cu}_3\text{SbSe}_4$  decreases with the increasing temperature, and after about 550 K, it shows a slight increase with increasing temperature. In contrast,  $S$  for samples with  $x=0.01$  and  $0.02$  decreases much slowly with increasing temperature and its value drops with increasing content of aluminum. This behavior is similar to that of the electrical resistivity, which also indicates that the Al-doped compounds become partially degenerate. Specially, one notices that  $S$  for sample with  $x = 0.03$  increases monotonically with temperature. This is the typically characteristic of a heavily degenerate semiconductor.

The temperature dependences of power factor  $\text{PF} (= S^2/\rho)$  of  $\text{Cu}_3\text{Sb}_{1-x}\text{Al}_x\text{Se}_4$  ( $x = 0, 0.01, 0.02$  and  $0.03$ ) are shown in Fig. 3(c). The values of PF for all the Al-doped compounds are larger than that for the un-doped one. Specially, the PF of sample with  $x = 0.03$  nearly increases linearly with temperature, and it reaches  $1.05 \times 10^{-3} \text{ W/(m}\cdot\text{K}^2)$  at 600 K, which is about twice as large as that of  $\text{Cu}_3\text{SbSe}_4$ .

The temperature dependences of the total thermal conductivity  $\kappa$ , lattice thermal conductivity  $\kappa_L$  and carrier contribution  $\kappa_c$  for  $\text{Cu}_3\text{Sb}_{1-x}\text{Al}_x\text{Se}_4$  ( $x = 0, 0.01, 0.02$  and  $0.03$ ) compounds are presented in Fig. 3(d) and Fig. 4, respectively. The results of the specific heat,  $C_p$ , determined by DSC for  $\text{Cu}_3\text{SbSe}_4$  from 300 K to 600 K are shown in Fig. 5. The values of  $C_p$  range from 0.31 to 0.37  $\text{Jg}^{-1}\text{K}^{-1}$ , which are in agreement with the result of Skoug et al.<sup>[9]</sup> but smaller than the data reported by Wei et al.<sup>[16]</sup>. As to Fig. 3(d), for all the samples,  $\kappa$  decreases with increasing temperature in the whole temperature range investigated. In comparison,  $\kappa$  of the Al-doped samples is slightly lower at room temperature and then becomes higher than that of the un-doped  $\text{Cu}_3\text{SbSe}_4$  with the increasing temperature due to the increased contribution from  $\kappa_c$  (the inset of Fig. 4). Lattice thermal conductivity  $\kappa_L$  is estimated by subtracting the carrier thermal conductivity  $\kappa_c$  from  $\kappa$ , where the Wiedemann-Franz relation with a Lorentz constant  $L_0$  is applied for estimating  $\kappa_c$  ( $\kappa_c = L_0 T/\rho$ ). Here,  $L_0$  is set to  $1.5 \times 10^{-8} \text{ V}^2\text{K}^{-2}$ ,  $2 \times 10^{-8} \text{ V}^2\text{K}^{-2}$  and  $2.44 \times 10^{-8} \text{ V}^2\text{K}^{-2}$  for a non-degenerate semiconductor ( $x = 0$ ), a partial degenerate semiconductor ( $x = 0.01, 0.02$ ) and a degenerate semiconductor ( $x = 0.03$ ), respectively<sup>[18,19]</sup>. As compared to the results of Wei et al.<sup>[17]</sup>, our lattice thermal conductivity  $\kappa_L$  (at 300 K) for un-doped one is around ~30% lower than that reported by Wei et al.<sup>[17]</sup>, which could, on the one hand, come partly from more porosities in our samples than theirs (the relative densities  $d_r$  for each sample are given in Table 1). On the other hand, the large number of dispersed nanoparticles (as shown in Fig. 2) will make great contribution to inhibiting lattice thermal conductivity of the bulk specimens due to extra phonon scattering at these nanoparticles, leading to smaller  $\kappa_L$ . As shown in Fig. 4,  $\kappa_L$  of samples with  $x = 0.01$  and  $0.02$  is similar to that of the un-doped sample. However,  $\kappa_L$  for  $x = 0.03$  is smaller than that of the pure sample especially at high temperatures.

RSC Advances Accepted Manuscript



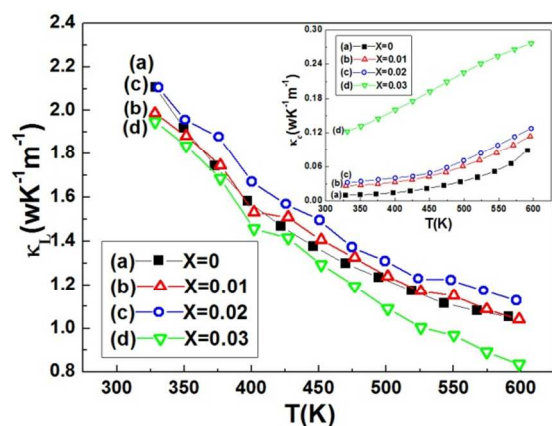


Fig. 4 Temperature dependences of the lattice thermal conductivity  $\kappa_L$  and the carrier thermal conductivity  $\kappa_c$  (the inset) for  $\text{Cu}_3\text{Sb}_{1-x}\text{Al}_x\text{Se}_4$ : (a)  $x = 0$ , (b)  $x = 0.01$ , (c)  $x = 0.02$  and (d)  $x = 0.03$ .

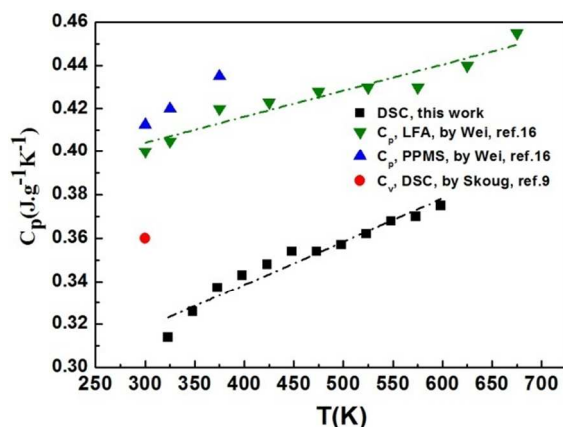


Fig. 5 Temperature dependences of the specific heat  $C_p$  determined by DSC for  $\text{Cu}_3\text{SbSe}_4$ .

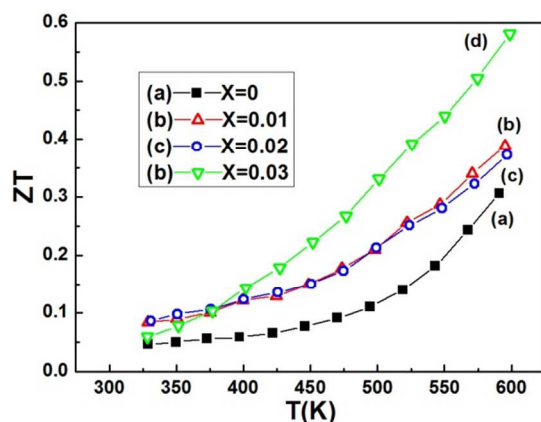


Fig. 6 Temperature dependence of ZT for  $\text{Cu}_3\text{Sb}_{1-x}\text{Al}_x\text{Se}_4$ : (a)  $x = 0$ , (b)  $x = 0.01$ , (c)  $x = 0.02$  and (d)  $x = 0.03$ .

Fig. 6 shows the temperature dependence of ZT for  $\text{Cu}_3\text{Sb}_{1-x}\text{Al}_x\text{Se}_4$  ( $x = 0, 0.01, 0.02$  and  $0.03$ ). ZT of the Al-doped compounds  $\text{Cu}_3\text{Sb}_{1-x}\text{Al}_x\text{Se}_4$  ( $x = 0.01, 0.02$  and  $0.03$ ) is larger than that of un-doped  $\text{Cu}_3\text{SbSe}_4$ . The maximum ZT reaches 0.58 for  $\text{Cu}_3\text{Sb}_{0.97}\text{Al}_{0.03}\text{Se}_4$  at 600 K, which is around 1.9 times as large as that of the un-doped  $\text{Cu}_3\text{SbSe}_4$  and is larger than the ZT value reported by Wei et al.<sup>[16]</sup> for Sn-doped  $\text{Cu}_3\text{SbSe}_4$  ( $\text{ZT} \approx 0.5$  at 600 K). The elevation of ZT for  $\text{Cu}_3\text{Sb}_{0.97}\text{Al}_{0.03}\text{Se}_4$  results mainly from both its enhanced PF due to the optimization of hole concentration and reduced  $\kappa_L$ .

#### 4. Conclusion

The effects of Al-doping on the thermoelectric properties of  $\text{Cu}_3\text{Sb}_{1-x}\text{Al}_x\text{Se}_4$  ( $x = 0, 0.01, 0.02$  and  $0.03$ ) compounds obtained by combining melting method with SPS are investigated in this work. Experiments show that Al-doping leads to large decreases in the electrical resistivity due to great increase in hole concentration. With increasing Al-doping content the samples transform from non-degenerate ( $x = 0$ ) to partial degenerate ( $x = 0.01, 0.02$ ) and then to degenerate state ( $x = 0.03$ ). PF of all the Al-doped samples is remarkably improved. Moreover, heavy Al-doping ( $x = 0.03$ ) leads to reduced lattice thermal conductivity. The largest  $\text{ZT}_{\text{max}} = 0.58$  is achieved at 600 K for  $\text{Cu}_3\text{Sb}_{0.97}\text{Al}_{0.03}\text{Se}_4$ , which is about 1.9 times larger than that of the un-doped compounds. Our study demonstrates that Al-doping is an effective and environment-friendly way to improve the thermoelectric performance of  $\text{Cu}_3\text{SbSe}_4$ .

#### Acknowledgments

Financial support from National Natural Science Foundation of China (Nos. 11174292, 11374306, 51101150, 50972146 and 10904144) is gratefully acknowledged.

\*Corresponding author. Tel: +86 0551 5592750; fax: +86 0551 5591434

E-mail address: [xyqin@issp.ac.cn](mailto:xyqin@issp.ac.cn), [lidi@issp.ac.cn](mailto:lidi@issp.ac.cn)

#### References

- [1] B.Poudel, Q.Hao, Y.Ma, Science, 2008, **320**, 634-638
- [2] J.P.Heremans, V.Jovovic, E.S.Toberer, Science, 2008, **321**, 554-557
- [3] M.L.Liu, I.W.Chen, F.Q.Huang, L.D.Chen, Adv Mater, 2009, **21**, 3808-3812
- [4] X.Shi, L.Xi, J.Fan, Chem Mater, 2010, **22**, 6029-6031
- [5] X.Y.Shi, F.Q.Huang, M.L.Liu, L.D.Chen, Appl Phys Lett, 2009, **94**, 122103
- [6] E.J.Skoug, J.D.Cain, D.T.Morelli, J Electron Mater, 2012, **41**, 1232-1236
- [7] D.Li, R.Li, X.Y.Qin, CrystEngComm, 2013, **15**, 7166
- [8] A.Suzumura, M.Watanabe, N.Nagasako, R.Asahi, J Electron Mater, 2014, **43**, 2356-2361.
- [9] E.J.Skoug, J.D.Cain, D.T.Morelli, Appl Phys Lett, 2011, **98**, 261911
- [10] E.J.Skoug, J.D.Cain, D.T.Morelli, J Appl Phys, 2011, **110**, 023501
- [11] T.R.Wei, F.Li, J.F.Li, J Electron Mater, 2014, **43**, 2229-2238
- [12] C.An, Q.Liu, K.Tang, J Crystal Growth, 2003, **256**, 128-133

- [13] C.Yang, F.Huang, L.Wu, K.Xu, J Phys D: Appl Phys, 2011, **44**, 295404
- [14] H.Katsumi, K.Masaru, Japanese J Appl Phys, 1968, **7**, 54-59
- [15] E.J.Skoug, J.D.Cain, P.Majsztrik, Sci Adv Mater, 2011, **3**, 602-606
- [16] T.R.Wei, H.Wang, Z.M.Gibbs, C.F.Wu, G.Jeffrey Snyder, J.F.Li, J Mater Chem A, 2014, **2**, 13527
- [17] X.Y.Li, D.Li, H.X.Xin, J Alloy Compd, 2013, **561**, 105-108
- [18] B.C.Sales, D.Mandrus, B.C.Chakoumakos, Phys Rev B, 1997, **56**, 23 ..
- [19] J.Zhang, H.J.Liu, L.Cheng, J Appl Phys, 2014, **116**, 023706.